Published in final edited form as:
J Proteome Res. 2014 February 7; 13(2): 1065–1076. doi:10.1021/pr4010579.

Metabolomics Analysis Identifies D-Alanine-D-alanine Ligase as the Primary Lethal Target of D-cycloserine in Mycobacteria

Steven Halouska[1], **Robert J. Fenton**[2], **Denise K. Zinniel**[2], **Darrell D. Marshall**[1], **Raúl G. Barletta**[2,3,*], and **Robert Powers**[1,2,*]

[1]Department of Chemistry, University of Nebraska-Lincoln, Lincoln, NE 68588-0304

[2]Redox Biology Center, University of Nebraska-Lincoln, Lincoln, NE 68583-0905

[3]School of Veterinary Medicine and Biomedical Sciences, University of Nebraska-Lincoln, Lincoln, NE 68583-0905

Abstract

D-cycloserine is an effective second line antibiotic used as a last resort to treat multi (MDR)- and extensively (XDR)- drug resistant strains of *Mycobacterium tuberculosis*. D-cycloserine interferes with the formation of peptidoglycan biosynthesis by competitive inhibition of Alanine racemase (Alr) and D-Alanine-D-alanine ligase (Ddl). Although, the two enzymes are known to be inhibited, the *in vivo* lethal target is still unknown. Our NMR metabolomics work has revealed that Ddl is the primary target of DCS, as cell growth is inhibited when the production of D-alanyl-D-alanine is halted. It is shown that inhibition of Alr may contribute indirectly by lowering the levels of D-alanine thus allowing DCS to outcompete D-alanine for Ddl binding. The NMR data also supports the possibility of a transamination reaction to produce D-alanine from pyruvate and glutamate, thereby bypassing Alr inhibition. Furthermore, the inhibition of peptidoglycan synthesis results in a cascading effect on cellular metabolism as there is a shift toward the catabolic routes to compensate for accumulation of peptidoglycan precursors.

Keywords

Tuberculosis; NMR metabolomics; mycobacteria; D-cycloserine

INTRODUCTION

Tuberculosis (TB) remains one of the leading causes of morbidity and mortality from a single infectious disease on a global perspective.[1] In 2011, 8.7 million people were infected with TB with over 1.8 million deaths world-wide. Moreover, the emergence of multiple- (MDR-TB) and extensively drug-resistant- (XDR-TB) *Mycobacterium tuberculosis* strains

Corresponding authors: Robert Powers, Department of Chemistry, 722 Hamilton Hall, University of Nebraska-Lincoln, Lincoln, NE 68588-0304, Tel: (402) 472-3039, Fax (402) 472-9402, rpowers3@unl.edu. Raúl G. Barletta, School of Veterinary, Medicine and Biomedical Sciences, 211 VBS, University of Nebraska-Lincoln, Lincoln NE 68583-0905, Tel. (402) 472-8543, Fax (402) 472-9690, rbarletta@unl.edu.

Author Contributions

R. G. B. and R. P. designed the research; S. H. performed NMR experiments and statistical analysis, D. D. M., R. J. F., and D. K. Z. prepared and analyzed the growth of the *M. smegmatis* and the *M. tuberculosis* cultures; S. H. and R. P. analyzed NMR and statistical data; S. H., D. K. Z., R. G. B. and R. P. analyzed metabolomics data; S. H., D. K. Z., R. G. B. and R. P. wrote the paper.

The authors declare no competing financial interest.

Supporting information

This material is available free of charge via the Internet at http://pubs.acs.org

threaten to curtail efforts in disease control. Currently, about 3.7% of new TB patients are infected with MDR-TB. A better understanding of the molecular mechanisms of action and resistance to existing antibiotics, and the development of novel drugs that are more potent and safer is urgently needed.

D-cycloserine (DCS) is a second line drug that is currently used as a last resort on MDR-and XDR-TB. DCS has been used to treat TB for over fifty years despite a lack of knowledge regarding the identity of its lethal target.[2] Although DCS inhibits bacterial cell growth, it has serious neurological side effects.[3–5] DCS treatment results in psychosis, depression, and convulsions, among other issues. In this context, DCS has also been tested in neurological studies and has been shown to act as a partial agonist of *N*-methyl-D-aspartate (NMDA) and glycine receptors.[6] Thus, understanding the source of DCS antimicrobial activity would enable the development of next-generation antibiotics for TB that avoids these CNS side effects. DCS is a cyclic analogue of D-alanine and has been shown to competitively inhibit Alanine racemase (Alr, EC 5.1.1.1) and D-alanine-D-alanine ligase (Ddl, EC 6.3.2.4).[7, 8] Correspondingly, the current understanding of DCS activity against mycobacteria is through the inhibition of Alr and/or Ddl that halts the synthesis of peptidoglycan precursors. However, we previously demonstrated that Alr is not the lethal target of DCS, suggesting Ddl is the primary target in live mycobacteria.[9] Moreover, we have now isolated new *alr* null mutants of *M. smegmatis* and *M. tuberculosis* that are not dependent for D-alanine under appropriate growth conditions, indicating that *alr* is not an essential gene in mycobacteria (unpublished results). This is also consistent with the observation by Takayama *et al.* that the UDP-MurNAc-tripeptide accumulates in *M. tuberculosis* upon treatment with DCS.[10] UDP-MurNAc-tripeptide is the product of the meso-diaminopimelate- adding enzyme (EC 6.3.2.13) in the peptidoglycan biosynthesis pathway, while the next step involves the MurF D-alanyl-D-alanine adding enzyme (EC 6.3.2.10) ligating the UDP-MurNAc-tripeptide with D-alanyl-D-alanine, the product of Ddl.[11] Clearly, the inhibition of Ddl by DCS would decrease the production of D-alanyl-D-alanine and lead to the observed accumulation of the UDP-MurNAc-tripeptide, as the co-substrate of the MurF reaction is decreased.

Peptidoglycan biosynthesis is an ideal target for drug design because the pathway is not present in mammalian cells.[11] Also, the resulting peptidoglycan-arabinogalactan complex gives the cell its structural integrity.[11–13] The peptidoglycan layer consists of an alternating N-acetylglucosamine and N-glycolated or N-acetylated muramic acid. Each N-glycolated or N-acetylated muramic acid is bound to a tetrapeptide consisting of an L-alanyl–D-isoglutaminyl–meso-diaminopimelyl–D-alanine (L-Ala–D-Glu–A_2pm–D-Ala) moiety. The tetrapeptide forms a crosslink between adjacent alternating aminosugars where the side chain of meso-diaminopimelate of one group forms a peptide bond with a D-alanine residue from the adjacent group. This large mycolyl-arabinogalactan-peptidoglycan complex creates an impermeable barrier that is essential for the viability of the cell.[14] This metabolic route includes the D-alanine branch pathway consisting of three enzymes that contribute to the synthesis of the glycomuramyl pentapeptide involved in the crosslinking of mature peptidoglycan. Alr is a pyridoxal phosphate dependent enzyme that interconverts L-alanine and D-alanine.[15, 16] The ATP Ddl catalyzes the subsequent peptide bond between two D-alanine moieties.[17] The final step is the addition of this dipeptide to the glycomuramyl tripeptide cytoplasmic precursor by the ATP-dependent MurF adding enzyme to form the pentapeptide complex.[18] As a result, numerous enzymes within the peptidoglycan biosynthesis machinery recognize or bind a D-alanine moiety and are potentially inhibited by DCS. Herein, we describe our application of Nuclear Magnetic Resonance (NMR) based metabolomics and bioinformatics to determine the lethal target of DCS in mycobacteria and to investigate the effects of this drug on central metabolic pathways related to peptidoglycan biosynthesis. Our analysis indicates that DCS is a promiscuous inhibitor targeting multiple

enzymes within the peptidoglycan biosynthesis pathway, but Ddl is the primary target. Our results also support the prior observation by Caceres *et al.*[19] that D-alanine is a competitive inhibitor of DCS and its over-production is a primary mechanism of resistance.

METHOD AND MATERIALS

Preparation of *M. tuberculosis* NMR Metabolomics Samples

General procedures for the handling and preparation of *M. tuberculosis* NMR samples for metabolomic analysis have been described elsewhere.[20] Six (3 for ^{13}C-D-alanine and 3 for ^{13}C-D-alanine DCS) *M. tuberculosis* H37Rv 110 mL MADC broth (Middlebrook 7H9 complete media) cultures from glycerol stock were grown shaking at 100 rpm at 37°C for approximately 7 days (OD_{600} 0.6–0.8). A 500 μl sample was removed and kept at 4°C for colony-forming unit (CFU) determinations. ^{13}C-D-alanine (0.1 mM final concentration; *e.g.* 100 μl of a 100 mM stock) was added to all cultures. DCS (50 μg/mL final concentration (500 μl of a 10 mg/mL stock)) was added to only 3 flasks. All cultures were incubated for an additional 18 hours, taking another OD_{600} reading and removing a 500 μl sample from each flask. Cultures were placed on ice for 5 minutes and left on ice throughout the rest of the processing. Cultures were harvested by spinning them down at 2000 g at 4°C for 15 minutes in 50 mL tubes. The samples were washed two times (~25–30 mL) with ice-cold double distilled water (ddH_2O). The cell pellets were resuspended with 1 mL of ddH_2O and transferred to a 2 mL vial consisting of 0.1 mm silica beads (Lysing Matrix B). The cells were then lysed using a FastPrep-24 instrument for 60 seconds at 6 m/s. The cellular mixture was centrifuged at 15,000 g at 4°C for 10 minutes and the supernatant was extracted to a 1.5 mL tube. 700 μl of ddH_2O was added to the tube containing the lysing matrix B and briefly vortexed, followed by centrifugation, and then transferring and combining the supernatants in a 1.5 mL tube. The supernatant was syringe filtered (0.2 Mm) into a sterile tube. A 100 Ml of the sample (10%) was plated on MADC to verify that there are no live cells. Samples were frozen in an EtOH-dry ice bath and stored at −80°C for 2 months. After verification that the plates contained no viable cells (CFUs), the metabolomic samples were taken out of BSL3 containment, lyophilized and prepared for analysis by NMR. 10 μL of the supernatant was used to determine protein concentration as described below for the *M. smegmatis* samples.

Preparation of *M. smegmatis* NMR Metabolomics Samples

NMR samples for 2D ^{1}H-^{13}C HSQC experiments were prepared from 6 groups of triplicate and independent *M. smegmatis* mc^{2}155 cultures using 100 μM $^{13}C_2$-D-alanine (^{13}Cα and ^{13}Cβ labeled) or $^{13}C_3$-pyruvate as a carbon-13 source. The following groups using $^{13}C_2$-D-alanine are mc^{2}155 as a control and mc^{2}155 treated with 75, 300, or 1200 μg/mL of DCS. The groups using $^{13}C_3$-pyruvate are untreated mc^{2}155 and mc^{2}155 treated with 75 μg/mL DCS. The replicate cultures were grown at 37°C with shaking at 200 rpm in 110 mL of MADC (250 mL flask) until an OD_{600} of 0.6 was met. $^{13}C_2$-D-alanine or $^{13}C_3$-pyruvate was inoculated to the designated cultures for a final concentration of 100 μM. The cultures were allowed to grow for 10 minutes and then were treated with DCS to a final concentration of 75, 300, or 1200 μg/mL. The cultures were then grown for an additional 2 hours before harvesting. Each culture was placed on ice for 5 minutes and then centrifuged for 10 minutes at 1500 g and 4°C. The cell pellets were washed twice with 30 mL of ice-cold ddH_2O. The cell pellets were re-suspended with 1 mL of ddH_2O and transferred to a 2 mL vial consisting of 0.1 mm silica beads. The cells were then lysed using a FastPrep-24 instrument for 40 seconds at 6 m/s. The cellular mixture was centrifuged for 10 minutes at 12,400 g and 4°C and the supernatant was extracted. 10 μL of the supernatant was used to determine the protein concentration in the extracted metabolomics sample. Bio-Rad DC Protein Assay was used to obtain the total protein concentration for each sample using bovine serum albumin as

a standard. The supernatant was frozen in a dry ice ethanol bath and stored at −80°C until analyzed by NMR.

Two groups of triplicate and independent *M. smegmatis* mc^2155 cultures were also grown using $^{13}C_6$-glucose as the carbon-13 source. The two groups are untreated mc^2155 and mc^2155 treated with 75 μg/mL DCS. The cell cultures were grown in 50 mL of minimal media containing 22 mM $^{13}C_6$-glucose, 500 mM ammonium chloride, and essential salts. The pH of the minimal media was adjusted to 7.2. The cultures were grown as described above until an OD_{600} of 0.6 was achieved. DCS was then added to the selected cultures to a concentration of 75 μg/mL and the bacteria were allowed to grow for 2 more hours. The metabolome was extracted as described above.

Prior to collecting the 2D ^1H-^{13}C HSQC spectra, all metabolomics samples are lyophilized and re-suspended in a 500 mM potassium phosphate buffer in 99.8% D_2O at a pH of 7.2 (uncorrected) containing 500 μM of unlabeled 3-(trimethylsilyl)-propionic-2,2,3,3-d_4 acid sodium salt (TMSP) as an internal standard. The volume used for each sample was normalized based on the relative protein concentration determined for each sample. The sample with the lowest protein concentration was dissolved in 650 μL of the NMR buffer, where the other samples were dissolved in a proportionally larger buffer volume based on the relative protein concentrations. In this manner, the final metabolomics sample concentrations were equivalent and directly comparable. 600 μL of the reconstituted metabolomics sample was then placed into a 5 mm NMR tube for data collection.

2D ^1H-^{13}C HSQC NMR Data Collection

The 2D ^1H-^{13}C HSQC NMR spectra were collected on a Bruker 500 MHz Avance DRX spectrometer equipped with a triple-resonance, Z-axis gradient cryoprobe. A BACS-120 sample changer with Bruker Icon software was used to automate the NMR data collection. All spectra were collected using the Time-Zero HSQC ($HSQC_0$) pulse sequence and followed the experimental protocol as previously described.[21] Briefly, the relative intensity of a peak in a standard 2D ^1H-^{13}C HSQC NMR spectrum is dependent on the metabolite concentration and a number of other factors, such as the magnitude of the J-coupling constant, relaxation processes and dynamics. Instead, the $HSQC_0$ experiment collects a series of three HSQC experiments with an increasing number of pulse sequence repetitions ($HSQC_1$, $HSQC_2$, $HSQC_3$). Correspondingly, the peak intensity will decrease proportionally with the number of pulse sequence repetitions due to the impact of J-coupling, relaxation, and other factors. Thus, the peak intensity can then be plotted as a function of the number of pulse sequence repetitions and extrapolated back to time-zero ($HSQC_0$). The peak intensity at time-zero is only dependent on metabolite concentration. The 2D ^1H-^{13}C HSQC NMR spectra were collected for 2 hours each with a total of 2048 data points and a spectrum width of 5000.0 Hz, and 64 data points with a spectrum width of 17607.23 Hz in the ^1H and ^{13}C dimensions, respectively. A total of 16 dummy scans, 128 scans, a receiver gain of 9195.2, and a relaxation delay of 1.5 seconds was used to obtain all spectra. A total of 109 2D ^1H-^{13}C HSQC NMR spectra were collected requiring approximately 218 hours of NMR spectrometer time to analyze the impact of DCS on *M. tuberculosis* and *M. smegmatis.*

2D ^1H-^{13}C HSQC NMR Data Analysis

All 2D NMR spectra were processed using the NMRpipe software package.[22] A reference spectrum for peak picking was created by adding all spectra together. All spectra including the reference spectra was automatically peak picked and the peak intensities were organized by their chemical shifts using NMRviewJ.[23] The observed NMR peaks were assigned to specific metabolites using ^1H and ^{13}C chemical shift tolerances of 0.05 and 0.40 ppm respectively. Metabominer,[24] Madison Metabolomics Consortium Database (MMCD),[25]

Human Metabolome Database (HMDB),[26] and Platform for Riken Metabolomics (PRIME)[27, 28] were used to identify all metabolites. All identified metabolites were verified using KEGG[29] and MetaCyc[30] databases.

The concentrations of all metabolites were calculated using an extrapolation procedure that has been previously described.[21] The concentration for each metabolite from the triplicate datasets are then averaged, standard deviation was calculated, and Student's t-tests were used to test for statistical significant ($p < 0.05$) differences between each group.

NMR Ligand Binding Assay for D-Alanine-D-alanine Ligase

M. tuberculosis D-Alanine-D-alanine ligase was obtained using protocols described previously.[17] Ligand binding assays were performed to determine if alanine, ATP, and DCS can bind to the ligase individually or in combination. Six combinations of each ligand were used: 1) ATP, 2) D-alanine 3) DCS, 4) ATP and D-alanine 5) ATP and DCS, and 6) ATP, D-alanine, and DCS. The final concentration for each ligand is 100 μM. A second set of the six combinations of ligands were prepared identically, but with the addition of 25 μM of D-Alanine-D-alanine ligase. NMR inhibition studies of the D-Alanine-D-alanine ligase were performed using multiple concentrations of D-alanine and DCS. A total of 4 mixtures were prepared using 100 μM D-alanine with 0, 250, 500, or 1000 μM DCS. ATP was kept at a high concentration of 6 mM to prevent any competitive inhibition by low ATP:ADP ratios. D-Alanine-D-alanine ligase was titrated into the solution for a final concentration of 25 μM.

Each of the NMR samples was dissolved in 600 μL of 50 mM Tris buffer (pH 8.0, uncorrected) consisting of 10 mM magnesium chloride, 11.1 μM TMSP, and 2% DMSO. 1D ^{1}H NMR spectra were collected using excitation sculpting to efficiently remove the solvent signal.[31] A total of 16k data points with a spectrum width of 5482.5 Hz were collected using 32 scans and 8 dummy scans. The acquisition time for each 1D ^{1}H NMR spectrum was approximately 5 minutes. A total of 34 1D ^{1}H NMR spectra were collected requiring approximately 170 minutes of NMR instrument time. The 1D ^{1}H NMR spectra were processed using ACD 1D NMR manager version 12.0. The peak area for D-alanine and D-alanyl-D-alanine was determined and the concentration was calculated based on the TMSP peak.

RESULTS

Overall Impact of DCS on *Mycobacterium smegmatis* and *Mycobacterium tuberculosis* Metabolomes

In our previous studies, we found that *M. smegmatis alr* null mutants were able to grow on Middlebrook 7H9 medium without D-alanine supplementation.[32, 33] Furthermore, principal component analysis (PCA) of NMR metabolomics data revealed that *M. smegmatis alr* null mutants had different clustering patterns in PCA scores plots than the wild type and resistant strains indicating that Alr inactivation had a major impact on the metabolome.[9] However, the wild type and *alr* mutant cells treated with DCS cluster together in the PCA scores plot, but separate from untreated *alr* mutant cells, indicating that DCS acts on a common target different from Alr. Also, the one-dimensional (1D) ^{1}H NMR metabolomics data showed that glutamate and pyruvate may be a source for D-alanine synthesis, suggesting that a transaminase may convert D-(L-)glutamate and pyruvate into D-alanine and α-ketoglutarate (Fig. 5). The heterologous racemization of amino acids by a bacterial transaminase has been previously observed.[34] Thus, Alr is not an essential function of mycobacteria and is not the lethal target of DCS. We hypothesized that the inhibition of a secondary target, possibly Ddl, may negatively impact cell survival and function as the lethal target.

To analyze in depth the mechanism of action of DCS in both *M. smegmatis* and *M. tuberculosis*, a comparison of the impact of DCS on both microorganisms was performed using NMR metabolomics (Fig. 1).Typically, metabolites from cell extracts are detectable by ^{1}H-NMR where the intensities of each peak correlate with the concentrations of the metabolites. Therefore, any differences in peak intensity between organisms indicate a difference in the metabolomes. A spectral comparison between these two species indicates that there are few differences in the metabolomes (Fig. 1a). More noticeable, the *M. tuberculosis* metabolome shows a higher concentration of carbohydrates and aminosugars (3.5–4.5 ppm). However, the impact of DCS is similar for both *M. smegmatis* and *M. tuberculosis* suggesting the mechanism of DCS inhibition is similar in both species. The 1D ^{1}H-NMR spectrum indicates that alanine (1.43–1.45 ppm) showed a large increase while glutamate (2.00–2.45 ppm) had a dramatic decrease in concentration when both *M. smegmatis* and *M. tuberculosis* were treated with DCS (highlighted by blue boxes). In *M. tuberculosis*, there is an increase in the concentration of UDP, acetate, α-ketoglutarate while there is a decrease in AMP, glutamine, and methionine (Fig. 1b). An increase in UDP would be expected because it is an important precursor for peptidoglycan synthesis by providing N-acetyl(glycolyl)-glucosamine and the corresponding muramate UDP-derivatives.

To further quantify metabolite changes resulting from DCS treatment, we collected 2D ^{1}H-^{13}C HSQC spectra after supplementing the bacterial growth medium with a carbon-13 source. This procedure allows for monitoring the carbon-13 flow through the metabolome. Since the natural abundance of carbon-13 is 1.1%, only compounds derived from the ^{13}C-labeled metabolite through enzymatic turnover will be detected in the 2D ^{1}H-^{13}C HSQC spectrum. As the D-alanine pathway is the primary focus of our study, both *M. smegmatis* and *M. tuberculosis* cells were pulse labeled with ^{13}C-D-alanine and treated with DCS shortly thereafter. Cells were further grown for approximately half to one generation and harvested. Not surprisingly, the resulting 2D ^{1}H-^{13}C HSQC spectrum of the metabolomes obtained from the two untreated mycobacterial species cells differed (Fig. 1 c,d). As observed in the 1D spectra, the *M. tuberculosis* peaks in the 2D ^{1}H-^{13}C HSQC spectrum appear to be more congested in the carbohydrate and aminosugar region (^{13}C = 60–80 ppm, ^{1}H = 3.0–4.5 ppm). Therefore, the carbon-13 flow for *M. tuberculosis* appears to be directed towards gluconeogenesis. This differs from *M. smegmatis*, where the peaks are well dispersed throughout the 2D ^{1}H-^{13}C HSQC spectrum and correspondingly in the metabolome.

Again, the impact of DCS appears to be similar for both *M. smegmatis* and *M. tuberculosis* as three additional peaks clearly appeared in both 2D ^{1}H-^{13}C HSQC spectra upon drug treatment (circled region in Fig. 1c,d). Using metabolomics databases containing reference NMR spectra, we were able to identify one of the peaks as alanine (^{13}Cα 56.0 ppm, ^{1}Hα 3.54 ppm). This is consistent with the inhibitory effect of DCS on Ddl that may lead to an accumulation of ^{13}C-D-alanine. However, the two nearby peaks were not identified from the NMR databases. Based on the peak intensities and chemical shifts, it was suspected to be a close derivative of D-alanine. To test this hypothesis, we collected the natural abundance spectrum of a solution of D-alanyl-D-alanine as a reference. The two unknown peaks were a perfect match to this D-alanyl-D-alanine reference spectrum (Fig. 1e) indicating that D-alanyl-D-alanine is accumulated upon DCS treatment with supplemental ^{13}C-D-alanine. This result was expected from Alr inhibition by DCS and the flow of the ^{13}C label into D-alanyl-D-alanine[35] as Ddl activity is maintained because the supplemented ^{13}C-D-alanine effectively competes with DCS for the Ddl active site.[19] Further inspection of cell growth curves confirmed that the DCS treated cultures when supplemented with ^{13}C-D-alanine were growing similarly to untreated cells. Thus, ^{13}C-D-alanine appears to compete very effectively with DCS and promote cell viability in the presence of DCS. This effect would readily explain the well-known reversal of DCS inhibition by D-alanine.[36]

Impact of DCS on the Central Metabolism and Peptidoglycan Synthesis

To study the impact of DCS on *M. smegmatis*, a detailed analysis of changes to the metabolome was performed by measuring the ^{13}C metabolite concentrations using 2D time-zero ^{1}H-^{13}C HSQC ($HSQC_0$) experiments.[21] Two sets of triplicate cultures were grown in minimal media with ^{13}C-glucose as the primary carbon source. Cells were grown to exponential phase, treated with 75 μg/mL of DCS and grown for one additional generation. Analysis of the corresponding cell extracts (Fig. 2a) indicated that the variations in the metabolites identified from the $HSQC_0$ experiment were similar to those identified from the 1D ^{1}H-NMR spectra (Fig. 1a,b). This further confirms that carbohydrate precursors leading towards the biosynthesis of trehalose, glycogen, rhamose and UDP-galactose were significantly decreased upon DCS treatment. Moreover, the increase in fructose-1,6-bisphosphate highlights the switch to the catabolic route suggesting up-regulation of the glycolytic pathway. Glutamate is an important metabolite for energy generation, purine synthesis, peptidoglycan synthesis, and transfer of amino groups. Consistent with these roles, glutamate was greatly decreased in the presence of DCS suggesting the metabolite was catabolized. This same catabolic effect was observed on the pools of nucleotide precursors such as dUMP, dCMP, dTDP, and thymidine, which were all decreased significantly upon DCS treatment. There is also a significant decrease in the concentration of precursors in the oxidative branch of the pentose phosphate pathway such as D-glucono-1,5-lactone and 6-phosphogluconate. But, there is also an increase in the concentration of D-ribose-5-phosphate and D-ribose, suggesting a switch to the non-oxidative branch of the pentose phosphate pathway.

β-alanine is the precursor of important vitamins such as panthotenate via the conversion of aspartate to β-alanine by the PanD enzyme. Moreover, pantothenate is a precursor of Coenzyme A, which is essential for the production of fatty acids and peptidoglycan. A significant decrease in the pool of β-alanine was also observed, potentially suggesting DCS may inhibit the PanD enzyme. Instead, the fluxes of carbon precursors is rerouted towards the production of methionine and lysine, the terminal product of the pantothenate pathway immediately downstream from meso-2-6-diaminopimelate, a component of the peptidoglycan bridge. However, the increase in concentration of N-alpha-acetyl-lysine suggests that lysine is also being catabolized. Other peptidoglycan precursors such as alanine, UDP-N-acetyl-glucosamine, UDP, D-ribose, D-ribose-5-phosphate, and carbamoyl-L-aspartate are all significantly increased, consistent with the inhibition of peptidoglycan biosynthesis.

These results were confirmed by a second metabolomics study using ^{13}C-pyruvate as a carbon-13 source (Fig. 2b). Carbon flow was initially directed toward gluconeogenesis and glutamate production. However, trehalose, myoinositol, glucose-1-phosphate and glutamate decreased significantly upon DCS treatment. Consistent with the inhibition of peptidoglycan synthesis, the fluxes of carbon precursors was also directed towards purine and lysine biosynthesis, as observed by the significant increase in UDP, N-carbamoyl-L-aspartate, and N-alpha-acetyl-lysine. There was also a significant increase in proline concentration as the metabolism of this amino acid plays an important role in the detoxification of methylglyoxal, a toxic aldehyde generated from the cleavage of the phosphate group of dihydroxyacetone phosphate by the enzyme methylglyoxal synthase.[37] The over production of methylglyoxal has been associated with the imbalance in the anabolic and catabolic processes in the cell.[38] Although we were unable to identify methylglyoxal, the increase in proline levels suggests the existence of a mechanism to compensate for excessive activity in the catabolic pathways.

Effect of D-alanine on DCS Inhibitory Activity

To determine the effect of DCS on the D-alanine pathway, *M. smegmatis* cultures were grown in Middlebrook 7H9 media supplemented with 100 μM ^{13}C-D-alanine at mid-exponential phase. After 10 min incubation, cultures were treated with either 75, 300, or 1200 μg/mL of DCS. To determine the uptake of ^{13}C-D-alanine, the total area under the peaks observed in the 2D ^{1}H-^{13}C HSQC spectra was compared between treated and untreated samples. This is possible because all of the peaks in the 2D ^{1}H-^{13}C HSQC spectrum are derived from ^{13}C-D-alanine. We observed that D-alanine was able to effectively compete with DCS for uptake. At 75 and 300 μg/mL the total carbon-13 concentration was approximately 35% higher in the DCS-treated cultures. This indicated that D-alanine uptake was increased as needed to produce peptidoglycan precursors and increase the internal D-alanine pools to out-compete DCS from internal targets such as Alr and Ddl. However, a 15% decrease in D-alanine uptake was observed at 1200 μg/mL DCS, which represents a 100-fold molar excess of DCS.

D-alanine readily reversed cell growth inhibition by DCS. For example, cell growth was inhibited when cultures were grown with ^{13}C-pyruvate and ^{13}C-glucose using 75 μg/mL DCS. Upon addition of 100 μM ^{13}C-D-alanine to the culture medium, growth inhibition was not observed even with 300 μg/mL DCS. Consistent cell growth inhibition only occurred when the DCS dosage was raised to 1200 μg/mL, a 100-fold molar excess of DCS to D-alanine (Fig. 3a). Comparison between non-inhibitory and inhibitory conditions was important to assess the transient effect of DCS on the metabolome (Fig. 3b). At 75 or 300 μg/mL DCS, the overall impact on the metabolome was minimal, as indicated by the corresponding heat maps of metabolite concentrations derived from ^{13}C-D-alanine (Fig. 3a). However, major changes were observed in cultures treated with 1200 μg/mL DCS, a concentration resulting in inhibition of both D-alanine uptake and cell growth.

Increasing the DCS concentration had a major impact on the pool of ^{13}C-labeled metabolites originating from ^{13}C-D-alanine (Fig. 4). At 75 μg/mL DCS, the internal pool of D-alanine increased 12-fold with respect to untreated culture. Similarly, a 4-fold increase in D-alanyl-D-alanine and a slight increase (10%) in glutamate were also observed. At 300 μg/mL DCS, the D-alanine concentration increased 4-fold compared to untreated cultures, while the D-alanyl-D-alanine and glutamate concentrations increased further by 5.5-fold and 50%, respectively. At 1200 μg/mL, both the D-alanine and D-alanyl-D-alanine concentrations were similar in both treated and untreated cultures, while the glutamate concentration decreased by 50%. Treatment with increasing DCS concentrations also leads to similar changes in other metabolite pools. For example, an increase in DCS concentration results in an increase in peptidoglycan precursors such as lysine and UDP. These results are consistent with the hypothesis that D-alanine can be metabolized by three pathways: i) direct stereospecific conversion into L-alanine by Alr, ii) dimerization into the peptidoglycan precursor D-alanyl-D-alanine by Ddl, and iii) transamination into pyruvate with concomitant formation of glutamate from α-ketoglutarate (Fig. 5). As pyruvate turnover is extremely fast (Fig. 2b), the rapid incorporation of the ^{13}C-label into glutamate may proceed in three steps: i) conversion of D-alanine into pyruvate, ii) pyruvate turnover into α-ketoglutarate, and finally iii) the incorporation of the ^{13}C-label into glutamate by iteration of the first step as required by the principle of microscopic reversibility. Thus, in absence of DCS, D-alanine is rapidly converted into L-alanine by Alr as well as other metabolites such as D-alanyl-D-alanine and glutamate. As the concentration of DCS is increased, Alr inhibition leads to label accumulation in the alanine pool, while the D-alanyl-D-alanine pool remains constant only decreasing at the higher DCS concentrations (1200 μg/mL) reflecting the inhibition of Ddl. Moreover, though the conversion of D-alanine into L-alanine is inhibited, the results indicate that part of this label is still converted into glutamate. These results suggest that

DCS first inhibits Alr, but cell growth inhibition parallels the inhibitory effect of DCS on Ddl. Moreover, there is a conversion of ^{13}C-D-alanine into ^{13}C-glutamate at all DCS concentrations, suggesting that a DCS-insensitive transaminase converts ^{13}C-D-alanine and α-ketoglutarate into ^{13}C-glutamate and ^{13}C-pyruvate (as shown in Fig. 5). By the principle of microscopic reversibility, this enzyme may also convert glutamate and pyruvate into D-alanine and α-ketoglutarate. Nonetheless, the major conversion of alanine and α-ketoglutarate into glutamate and pyruvate depends on a transaminase that uses L-alanine as a substrate (*e.g.*, EC 2.6.1.2), as the ^{13}C-label incorporated into glutamate decreases significantly upon Alr inhibition. Therefore, Ddl rather than Alr, is the main lethal target of DCS, while a transaminase that uses (D-(L-) glutamate as substrates is responsible for the alternative pathway of D-alanine biosynthesis (Fig. 5). It is important to note that other enzymatic reactions that produce D-alanine are possible alternative explanations, such as the Strickland reaction in the ornithine fermentation pathway[39] or the decarboxylation of D-(L-)-aspartate by a broad range D-amino acid transaminase (EC 2.6.1.21).[40] Correspondingly, the observed PanD inhibition and decrease in β-alanine caused by DCS may result from an increase in the production of CoA for the Strickland reaction. Of course, the ornithine fermentation pathway that is composed of nine enzymes has not been identified in mycobacteria. Alternatively, the observed increase in aspartate upon DCS treatment may suggest D-aspartate is being converted into D-alanine through the activity of a D-amino acid transaminase that uses D-(L-)-aspartate as substrates for decarboxylation. Nevertheless, this still requires invoking the activity of a transaminase to explain the production of D-alanine when Alr is inhibited by DCS.

There are many classes of transaminases that have been identified in bacteria, such as: Aspartate transaminase (EC 2.6.1.1), Alanine transaminase (EC 2.6.1.2), 4-Aminobutyrate-2-oxoglutarate transaminase (EC 2.6.1.19), D-amino acid (broad-range)/D-Alanine transaminase (EC 2.6.1.21), and the branched-chain-amino acid transaminase (EC 2.6.1.42). Candidate genes for all of these enzymes, except D-amino acid transaminase, have been identified in *M. smegmatis* and *M. tuberculosis* (Table 1). There are 26 additional aminotransferases in the *M. tuberculosis* genome, with 8 being described as “probable aminotransferase” without an assigned function.

Canonical D-Alanine transaminases have been found in Gram-negative proteobacteria (*Brucella*, *Legionella*, *Rhodobacter*), and Gram-positive firmicutes (*Bacillus*, *Enterococcus*, *Lactobacillus*, *Listeria*, *Staphylococcus*) based on information from the NCBI Protein Database.[41, 42] However, mycobacteria are weakly Gram-positive and have high GC genome contents which is quite different from the major group of Gram-positive microorganisms in the phylogenetic tree. Thus, it is not surprising that a homologous D-alanine transaminase has not been identified in mycobacterial genomes. But using this lack of homology to conclude that D-alanine transaminase is not present in mycobacteria is premature.[43] Aminotransferases are well-known to have relaxed substrate specificity and as a result are increasingly used in the biosynthesis of challenging pharmaceuticals.[44–46] Thus, the mycobacterial genomes may still encode a non-homologous protein that can perform this transamination reaction. In effect, the biochemical property of each aminotransferase needs to be thoroughly assessed before a specific enzymatic activity can be excluded. For instance, a D-amino acid transaminase has been identified in *Listeria monocytogenes* that provides an alternative route of D-alanine biosynthesis.[47] A Delta-Blast[48] search using the *L. monocytogenes* D-amino acid transaminase sequence identified two homologous proteins in *M. smegmatis* and *M. tuberculosis*. While these proteins have been assigned to other functions, it is still plausible that one of these proteins is involved in a transamination reaction yielding D-alanine. Similarly, any of the probable aminotransferases present in the *M. tuberculosis* genome may also be a D-amino acid transaminase.

Impact of DCS on D-Alanine-D-alanine Ligase

To further investigate the interaction of DCS and the Ddl lethal target, the binding of relevant potential ligands with Ddl were followed by NMR. Moreover, the influence of a given ligand on the simultaneous or consecutive binding of another ligand was followed as well. Previous studies have yielded dissimilar results regarding the dependency of D-alanine binding on the presence of ATP in solution.[8, 17] However, Prosser *et al.* used a D-alanine ligase recombinant protein containing the intact polyhistidine tag that could have introduced undesirable interactions. To resolve this issue, purified untagged Ddl was incubated with ATP, D-alanine, or both ATP and D-alanine and binding was analyzed by NMR (Figs. 1S–3S). The observed NMR peak broadening for ATP upon the addition of Ddl indicates that ATP binds strongly to Ddl in the absence of D-alanine. Conversely, the D-alanine NMR peaked is unaffected by the addition of Ddl in the absence of ATP, indicating that D-alanine cannot bind to Ddl without ATP. The addition of ATP induces the binding of D-alanine to Ddl and the conversion of D-alanine to D-alanyl-D-alanine and ATP to ADP (Fig. 4S). These results are consistent with the mechanism of ordered binding and the binding assays reported by Prosser and de Carvalho with the polyhistidine tagged enzyme.[8] The experiments reported by Bruning *et al.* with the same untagged Ddl enzyme used in our study, may have revealed a different Ddl conformation than the one assessed by our NMR studies.

1D ^{1}H-NMR line-broadening binding assays were also carried out with DCS, DCS and ATP, and DCS with both ATP and D-alanine. The DCS NMR peaks broaden and incurred a chemical shift change in all three cases indicating that, in contrast to D-alanine, DCS can bind Ddl independently of ATP. Nonetheless, DCS is a weak binding ligand as evident by the modest changes in line-width and chemical shifts consistent with reported K_i values of 14 μM[8] to 0.9 mM.[49]

To confirm these results, we followed the progression of the Ddl (25 μM) reaction at varying DCS concentrations and fixed amounts of D-alanine (100 μM) and ATP (100 μM). Using NMR, the concentrations of the substrates (ATP and D-alanine) and two of the products (ADP and D-alanyl- D-alanine) were determined over time (Fig. 4S). In the absence of DCS, the conversion of ATP and D-alanine into ADP and D-alanyl-D-alanine was stoichiometric, but followed a very slow kinetics, reaching a maximum conversion in the forward reaction at approximately 4 h (Fig. 6a). Thereafter, the reaction was inhibited by accumulation of the ADP and D-alanyl-D-alanine products. To analyze the inhibitory effect of DCS, the reaction conditions were modified by adding saturating amounts of ATP at 6.0 mM. Under these conditions, the reaction proceeds to completion until D-alanine is exhausted (Fig. 6b). At increasing DCS concentrations, the reaction is progressively inhibited, but never reaches full inhibition. This is as expected given that DCS binds weakly to Ddl and D-alanine is a competitor of DCS.

DISCUSSION

DCS is known to inhibit peptidoglycan biosynthesis, but its primary target has been a point of controversy and extensive investigation for over fifty years. The effect of DCS has been attributed to the inhibition of Alr, Ddl or both.[32, 33, 43, 50] Both Alr and Ddl are known binding targets in mycobacteria and their enzymatic activities are inhibited by DCS in a concentration dependent manner.[19, 35] Alr is the only known enzyme to produce D-alanine in *M. smegmatis* and *M. tuberculosis.* In addition, previous studies have shown that the overexpression of *alr* confers resistance to DCS while *alr* mutant strains are more susceptible.[19, 33] However, overexpression of *ddl* also leads to DCS resistance, but to lower levels.[35] Similarly, contradictory genetic studies have been presented that seem to indicate that Alr is required in the absence of D-alanine.[43, 50] Nonetheless, as we have previously

observed,[19] these seemingly contradictory results may occur because of the different experimental conditions employed by these various studies to analyze Alr conditional essentiality. Critically, *alr* mutants are still able to grow in the absence of D-alanine. [32, 33] Also, the NMR metabolomic profiles of *alr* mutants do not match the metabolome of wild type *M. smegmatis* treated with DCS, which indicates that Alr is not the main inhibitory target of DCS.[9] Thus, these studies taken together conclusively rule out Alr as the lethal target of DCS in mycobacteria.

In this study, we found that DCS does not only inhibit peptidoglycan synthesis, but it also caused a cascade of effects on the central metabolism of the cell (Fig. 7). Our NMR metabolomics results using both ^{13}C-glucose and ^{13}C-pyruvate as carbon-13 sources showed a large increase in the accumulation of peptidoglycan precursors, as would be expected from DCS inhibition of peptidoglycan biosynthesis. Furthermore, DCS treatment of both *M. smegmatis* and *M. tuberculosis* resulted in a metabolic shift towards a catabolic state. We hypothesize that this catabolic shift occurs to compensate for the need to increase the synthesis of peptidoglycan precursors used to construct the cell wall. The shift towards the non-oxidative branch of the pentose phosphate pathway was evidenced by a decrease in oxidative branch metabolites with a concomitant increase in ribose-5-phosphate. This effect is most likely associated with the inhibition of peptidoglycan synthesis as ribose-5-phosphate is used in the synthesis of UTP needed to generate UDP-N-acetyl-glucosamine, which is the initial precursor in this biosynthetic step. This metabolic shift is also likely to result in a decrease in mycolic acid formation since the pentose phosphate oxidative branch is a major source of NADPH, which is required for the synthesis of mycolic and fatty acids. This would be expected to further weaken the cell wall and contribute to the bactericidal action of DCS.

The demonstration that a decrease in the biosynthesis of D-alanyl-D-alanine occurs simultaneously with cell growth inhibition shows that Ddl is the primary target of DCS. However, inhibition of Alr may contribute indirectly to the effect of DCS by simply lowering the pools of D-alanine produced.[32] The lower levels of D-alanine upon Alr inactivation may allow DCS to outcompete D-alanine for Ddl binding. However the inactivation of Alr would not prevent the cells from obtaining D-alanine from an alternative pathway by transamination from pyruvate with concomitant production of glutamate as we report here and elsewhere.[9, 32, 33] Other investigators proposed that Alr, rather than Ddl, is the main target of DCS based on the reversal of growth inhibition by externally added D-alanine and the weak reversal activity of D-alanyl-D-alanine. [50] However, our results clearly show that D-alanine and DCS are both competitors for Ddl binding, where a significant increase in D-alanine concentration can mitigate DCS activity by the intracellular protection of Ddl. Ddl is simply a kinetically inefficient enzyme and, correspondingly, a bottle neck in peptidoglycan biosynthesis. The externally added D-alanine is simply increasing Ddl activity by outcompeting DCS. Thus, increasing the intracellular pool of D-alanine is an effective mechanism of increasing DCS resistance. Thus, our combined analysis in this and previous studies indicate that DCS acts primarily on Ddl, an alternative pathway provides a source of D-alanine when Alr activity is inhibited or deleted, and Alr plays an indirect role in protecting Ddl by maintaining a higher internal pool of D-alanine. Importantly, these insights will help guide future drug discovery efforts.

DCS is commonly used as a second-line treatment of drug-resistant TB despite its serious side effects. These side effects are attributed to off-target activity and are consistent with our NMR metabolomics study where DCS inhibits multiple targets *in vivo*. Correspondingly, our identification that D-alanine-D-alanine ligase is the lethal target of DCS will support the future design of DCS-derived drugs with reduced side effects. Simply, drug discovery efforts can be focused on developing next-generation TB drugs by designing compounds

that selectively inhibit D-alanine-D-alanine ligase. Furthermore, our detailed analysis of changes in the metabolome due to DCS treatment will also be invaluable for validating the desired *in vivo* activity of next-generation Ddl inhibitors. Selective inhibitors of Ddl should induce metabolome perturbations comparable to DCS. Finally, our metabolomics study identified that the over-production of D-alanine is a simple and effective mechanism of resistance against Ddl inhibitors. Thus, a combination therapy for a DCS-derived drug may be a more effective TB therapy; a Ddl inhibitor should be supplemented with inhibitors of Alr and the predicted transaminase to prevent resistance. In conclusion, our detailed metabolomics study resolved a 50-year old mystery regarding the *in vivo* lethal target of DCS and laid the foundation for developing new TB therapies based on DCS and Ddl.

Supplementary Material

Refer to Web version on PubMed Central for supplementary material.

Acknowledgments

This manuscript was supported in part by funds from the National Institute of Health (AI087668, P20 RR-17675, P30 GM103335), the USDA NIFA Station Animal Health Project (NEB 39-162), the American Heart Association (0860033Z), the UNL School of Veterinary Medicine and Biomedical Sciences, and the Nebraska Research Council. S. Halouska and R. J. Fenton were partially supported by O. Chacon's NIH grant (R21 AI087561) to standardize NMR techniques included in this publication. The research was performed in facilities renovated with support from the National Institutes of Health (RR015468-01). We thank Drs. John Bruning and James Sacchettini from Texas A&M University for the kind gift of the purified Ddl used in the binding assays.

References

1. World Health Organization. Global Tuberculosis Report 2012. World Health Organization; Geneva, Switzerland: 2012. p. 100
2. Zhang Y. The magic bullets and tuberculosis drug targets. Annu Rev Pharmacol Toxicol. 2005; 45:529–64. [PubMed: 15822188]
3. Mitnick CD, Shin SS, Seung KJ, Rich ML, Atwood SS, Furin JJ, Fitzmaurice GM, Alcantara Viru FA, Appleton SC, Bayona JN, Bonilla CA, Chalco K, Choi S, Franke MF, Fraser HS, Guerra D, Hurtado RM, Jazayeri D, Joseph K, Llaro K, Mestanza L, Mukherjee JS, Munoz M, Palacios E, Sanchez E, Sloutsky A, Becerra MC. Comprehensive treatment of extensively drug-resistant tuberculosis. New Engl J Med. 2008; 359(6):563–74. [PubMed: 18687637]
4. Cunha BA. Antibiotic side effects. Med Clin North Am. 2001; 85(1):149–85. [PubMed: 11190350]
5. Torun T, Gungor G, Ozmen I, Bolukbasi Y, Maden E, Bicakci B, Atac G, Sevim T, Tahaoglu K. Side effects associated with the treatment of multidrug-resistant tuberculosis. Int J Tuberc Lung Dis. 2005; 9(12):1373–7. [PubMed: 16468160]
6. Hood WF, Compton RP, Monahan JB. D-cycloserine: a ligand for the N-methyl-D-aspartate coupled glycine receptor has partial agonist characteristics. Neurosci Lett. 1989; 98(1):91–5. [PubMed: 2540460]
7. Lambert MP, Neuhaus FC. Mechanism of D-cycloserine action: alanine racemase from Escherichia coli W. J Bacteriol. 1972; 110(3):978–87. [PubMed: 4555420]
8. Prosser GA, de Carvalho LP. Kinetic mechanism and inhibition of Mycobacterium tuberculosis D-alanine:D-alanine ligase by the antibiotic D-cycloserine. The FEBS J. 2013; 280(4):1150–66.
9. Halouska S, Chacon O, Fenton RJ, Zinniel DK, Barletta RG, Powers R. Use of NMR metabolomics to analyze the targets of D-cycloserine in mycobacteria: Role of D-alanine racemase. J Proteome Res. 2007; 6(12):4608–4614. [PubMed: 17979227]
10. Takayama K, David HL, Wang L, Goldman DS. Isolation and characterization of uridine diphosphate-N-glycolylmuramyl-L-alanyl-gamma-D-glutamyl-meso-alpha, alpha'-diamino pimelic acid from Mycobacterium tuberculosis. Biochem Biophys Res Commun. 1970; 39(1):7–12. [PubMed: 4985610]

11. Lovering AL, Safadi SS, Strynadka NC. Structural perspective of peptidoglycan biosynthesis and assembly. Annu Rev Biochem. 2012; 81:451–78. [PubMed: 22663080]
12. Crick DC, Mahapatra S, Brennan PJ. Biosynthesis of the arabinogalactan-peptidoglycan complex of Mycobacterium tuberculosis. Glycobiology. 2001; 11(9):107R–118R.
13. Vollmer W, Blanot D, de Pedro MA. Peptidoglycan structure and architecture. FEMS Microbiol Rev. 2008; 32(2):149–67. [PubMed: 18194336]
14. de Souza MVN, Ferreira MD, Pinheiro AC, Saraiva MF, de Almeida MV, Valle MS. Synthesis and biological aspects of mycolic acids: An important target against Mycobacterium tuberculosis. Scientific World Journal. 2008; 8:720–751. [PubMed: 18677428]
15. Strych U, Penland RL, Jimenez M, Krause KL, Benedik MJ. Characterization of the alanine racemases from two mycobacteria. FEMS Microbiol Lett. 2001; 196(2):93–8. [PubMed: 11267762]
16. LeMagueres P, Im H, Ebalunode J, Strych U, Benedik MJ, Briggs JM, Kohn H, Krause KL. The 1. 9 A crystal structure of alanine racemase from Mycobacterium tuberculosis contains a conserved entryway into the active site. Biochemistry. 2005; 44(5):1471–81. [PubMed: 15683232]
17. Bruning JB, Murillo AC, Chacon O, Barletta RG, Sacchettini JC. Structure of the Mycobacterium tuberculosis D-alanine:D-alanine ligase, a target of the antituberculosis drug D-cycloserine. Antimicrob Agents Chemother. 2011; 55(1):291–301. [PubMed: 20956591]
18. El Zoeiby A, Sanschagrin F, Levesque RC. Structure and function of the Mur enzymes: development of novel inhibitors. Mol Microbiol. 2003; 47(1):1–12. [PubMed: 12492849]
19. Caceres NE, Harris NB, Wellehan JF, Feng Z, Kapur V, Barletta RG. Overexpression of the D-alanine racemase gene confers resistance to D-cycloserine in Mycobacterium smegmatis. J Bacteriol. 1997; 179(16):5046–55. [PubMed: 9260945]
20. Zinniel DK, Fenton RJ, Halouska S, Powers R, Barletta RG. Sample Preparation of Mycobacterium tuberculosis Extracts for Nuclear Magnetic Resonance (NMR) Metabolomic Studies. J Vis Exp. 2012; 67:e3673. [PubMed: 22971839]
21. Hu KF, Westler WM, Markley JL. Simultaneous Quantification and Identification of Individual Chemicals in Metabolite Mixtures by Two-Dimensional Extrapolated Time-Zero H-1-C-13 HSQC (HSQC(0)). J Amer Chem Soc. 2011; 133(6):1662–1665. [PubMed: 21247157]
22. Delaglio F, Grzesiek S, Vuister GW, Zhu G, Pfeifer J, Bax A. NMRPipe: a multidimensional spectral processing system based on UNIX pipes. J Biomol NMR. 1995; 6(3):277–93. [PubMed: 8520220]
23. Johnson BA. Using NMRView to visualize and analyze the NMR spectra of macromolecules. Methods Mol Biol. 2004; 278:313–52. [PubMed: 15318002]
24. Xia J, Bjorndahl TC, Tang P, Wishart DS. MetaboMiner--semi-automated identification of metabolites from 2D NMR spectra of complex biofluids. BMC Bioinf. 2008; 9:507.
25. Cui Q, Lewis IA, Hegeman AD, Anderson ME, Li J, Schulte CF, Westler WM, Eghbalnia HR, Sussman MR, Markley JL. Metabolite identification via the Madison Metabolomics Consortium Database. Nat Biotechnol. 2008; 26(2):162–164. [PubMed: 18259166]
26. Wishart DS, Jewison T, Guo AC, Wilson M, Knox C, Liu Y, Djoumbou Y, Mandal R, Aziat F, Dong E, Bouatra S, Sinelnikov I, Arndt D, Xia J, Liu P, Yallou F, Bjorndahl T, Perez-Pineiro R, Eisner R, Allen F, Neveu V, Greiner R, Scalbert A. HMDB 3.0--The Human Metabolome Database in 2013. Nucleic Acids Res. 2013; 41(Database issue):D801–7. [PubMed: 23161693]
27. Sakurai T, Yamada Y, Sawada Y, Matsuda F, Akiyama K, Shinozaki K, Hirai MY, Saito K. PRIMe Update: Innovative Content for Plant Metabolomics and Integration of Gene Expression and Metabolite Accumulation. Plant Cell Physiol. 2013; 54(2):e5. [PubMed: 23292601]
28. Akiyama K, Chikayama E, Yuasa H, Shimada Y, Tohge T, Shinozaki K, Hirai MY, Sakurai T, Kikuchi J, Saito K. PRIMe: a Web site that assembles tools for metabolomics and transcriptomics. In silico biology. 2008; 8(3–4):339–45. [PubMed: 19032166]
29. Kanehisa M, Araki M, Goto S, Hattori M, Hirakawa M, Itoh M, Katayama T, Kawashima S, Okuda S, Tokimatsu T, Yamanishi Y. KEGG for linking genomes to life and the environment. Nucleic Acids Res. 2008; 36(Database):D480–D484. [PubMed: 18077471]
30. Caspi R, Foerster H, Fulcher CA, Kaipa P, Krummenacker M, Latendresse M, Paley S, Rhee SY, Shearer AG, Tissier C, Walk TC, Zhang P, Karp PD. The MetaCyc Database of metabolic

pathways and enzymes and the BioCyc collection of Pathway/Genome Databases. Nucleic Acids Res. 2008; 36(Database issue):D623–31. [PubMed: 17965431]

31. Nguyen BD, Meng X, Donovan KJ, Shaka AJ. SOGGY: solvent-optimized double gradient spectroscopy for water suppression. A comparison with some existing techniques. J Magn Reson. 2007; 184(2):263–74. [PubMed: 17126049]
32. Chacon O, Bermudez LE, Zinniel DK, Chahal HK, Fenton RJ, Feng Z, Hanford K, Adams LG, Barletta RG. Impairment of D-alanine biosynthesis in Mycobacterium smegmatis determines decreased intracellular survival in human macrophages. Microbiology. 2009; 155(Pt 5):1440–50. [PubMed: 19383714]
33. Chacon O, Feng Z, Harris NB, Caceres NE, Adams LG, Barletta RG. Mycobacterium smegmatis D-alanine racemase mutants are not dependent on D-alanine for growth. Antimicrob Agents Chemother. 2002; 46(1):47–54. [PubMed: 11751110]
34. Martinez, dPA.; Merola, M.; Ueno, H.; Manning, JM.; Tanizawa, K.; Nishimura, K.; Soda, K.; Ringe, D. Stereospecificity of reactions catalyzed by bacterial D-amino acid transaminase. J Biol Chem. 1989; 264(30):17784–9. [PubMed: 2808352]
35. Feng Z, Barletta RG. Roles of Mycobacterium smegmatis D-alanine:D-alanine ligase and D-alanine racemase in the mechanisms of action of and resistance to the peptidoglycan inhibitor D-cycloserine. Antimicrob Agents Chemother. 2003; 47(1):283–91. [PubMed: 12499203]
36. Zygmunt WA. Antagonism of D-cycloserine inhibition of mycobacterial growth by D-alanine. J Bacteriol. 1963; 85:1217–20. [PubMed: 14047211]
37. Berney M, Weimar MR, Heikal A, Cook GM. Regulation of proline metabolism in mycobacteria and its role in carbon metabolism under hypoxia. Mol Microbiol. 2012; 84(4):664–81. [PubMed: 22507203]
38. Freedberg WB, Kistler WS, Lin EC. Lethal synthesis of methylglyoxal by Escherichia coli during unregulated glycerol metabolism. J Bacteriol. 1971; 108(1):137–44. [PubMed: 4941552]
39. Fonknechten N, Perret A, Perchat N, Tricot S, Lechaplais C, Vallenet D, Vergne C, Zaparucha A, Le PD, Weissenbach J, Salanoubat M. A conserved gene cluster rules anaerobic oxidative degradation of L-ornithine. J Bacteriol. 2009; 191(9):3162–3167. [PubMed: 19251850]
40. Jones WM, Van OPW, Pospischil MA, Ringe D, Petsko G, Soda K, Manning JM. The ubiquitous cofactor NADH protects against substrate-induced inhibition of a pyridoxal enzyme. Protein Sci. 1996; 5(12):2545–2551. [PubMed: 8976563]
41. Wheeler DL, Church DM, Federhen S, Lash AE, Madden TL, Pontius JU, Schuler GD, Schriml LM, Sequeira E, Tatusova TA, Wagner L. Database resources of the national center for biotechnology. Nucleic Acids Res. 2003; 31(1):28–33. [PubMed: 12519941]
42. Pruitt KD, Tatusova T, Maglott DR. NCBI Reference Sequence (RefSeq): a curated non-redundant sequence database of genomes, transcripts and proteins. Nucleic Acids Res. 2005; 33(Database):D501–D504. [PubMed: 15608248]
43. Milligan DL, Tran SL, Strych U, Cook GM, Krause KL. The alanine racemase of Mycobacterium smegmatis is essential for growth in the absence of D-alanine. J Bacteriol. 2007; 189(22):8381–8386. [PubMed: 17827284]
44. Rudat J, Brucher BR, Syldatk C. Transaminases for the synthesis of enantiopure beta-amino acids. AMB Express. 2012; 2(1):11, 10. [PubMed: 22293122]
45. Stewart JD. Dehydrogenases and transaminases in asymmetric synthesis. Curr Opin Chem Biol. 2001; 5(2):120–129. [PubMed: 11282337]
46. Taylor PP, Pantaleone DP, Senkpeil RF, Fotheringham IG. Novel biosynthetic approaches to the production of unnatural amino acids using transaminases. Trends Biotechnol. 1998; 16(10):412–418. [PubMed: 9807838]
47. Thompson RJ, Bouwer HGA, Portnoy DA, Frankel FR. Pathogenicity and immunogenicity of a Listeria monocytogenes strain that requires D-alanine for growth. Infect Immun. 1998; 66(8): 3552–3561. [PubMed: 9673233]
48. Boratyn GM, Schaffer AA, Agarwala R, Altschul SF, Lipman DJ, Madden TL. Domain enhanced lookup time accelerated BLAST. Biol Direct. 2012; 7:12. [PubMed: 22510480]
49. Neuhaus, FC. D-Cycloserine and O-Carbamyl-D-serine. In: Gottlieb, D.; Shaw, PD., editors. Mechanism of Action. Vol. 1. Springer; Berlin Heidelberg: 1967. p. 40-83.

50. Awasthy D, Bharath S, Subbulakshmi V, Sharma U. Alanine racemase mutants of Mycobacterium tuberculosis require D-alanine for growth and are defective for survival in macrophages and mice. Microbiology. 2012; 158(Pt 2):319–27. [PubMed: 22075031]

51. Lew JM, Kapopoulou A, Jones LM, Cole ST. TubercuList--10 years after. Tuberculosis. 2011; 91(1):1–7. [PubMed: 20980199]

52. Kohanski MA, Dwyer DJ, Collins JJ. How antibiotics kill bacteria: from targets to networks. Nat Rev Microbiol. 2010; 8(6):423–435. [PubMed: 20440275]

53. Mahapatra S, Scherman H, Brennan PJ, Crick DC. N Glycolylation of the nucleotide precursors of peptidoglycan biosynthesis of Mycobacterium spp. is altered by drug treatment. J Bacteriol. 2005; 187(7):2341–7. [PubMed: 15774877]

54. de Roubin MR, Mengin-Lecreulx D, van Heijenoort J. Peptidoglycan biosynthesis in Escherichia coli: variations in the metabolism of alanine and D-alanyl-D-alanine. J Gen Microbiol. 1992; 138(Pt 8):1751–7. [PubMed: 1527514]

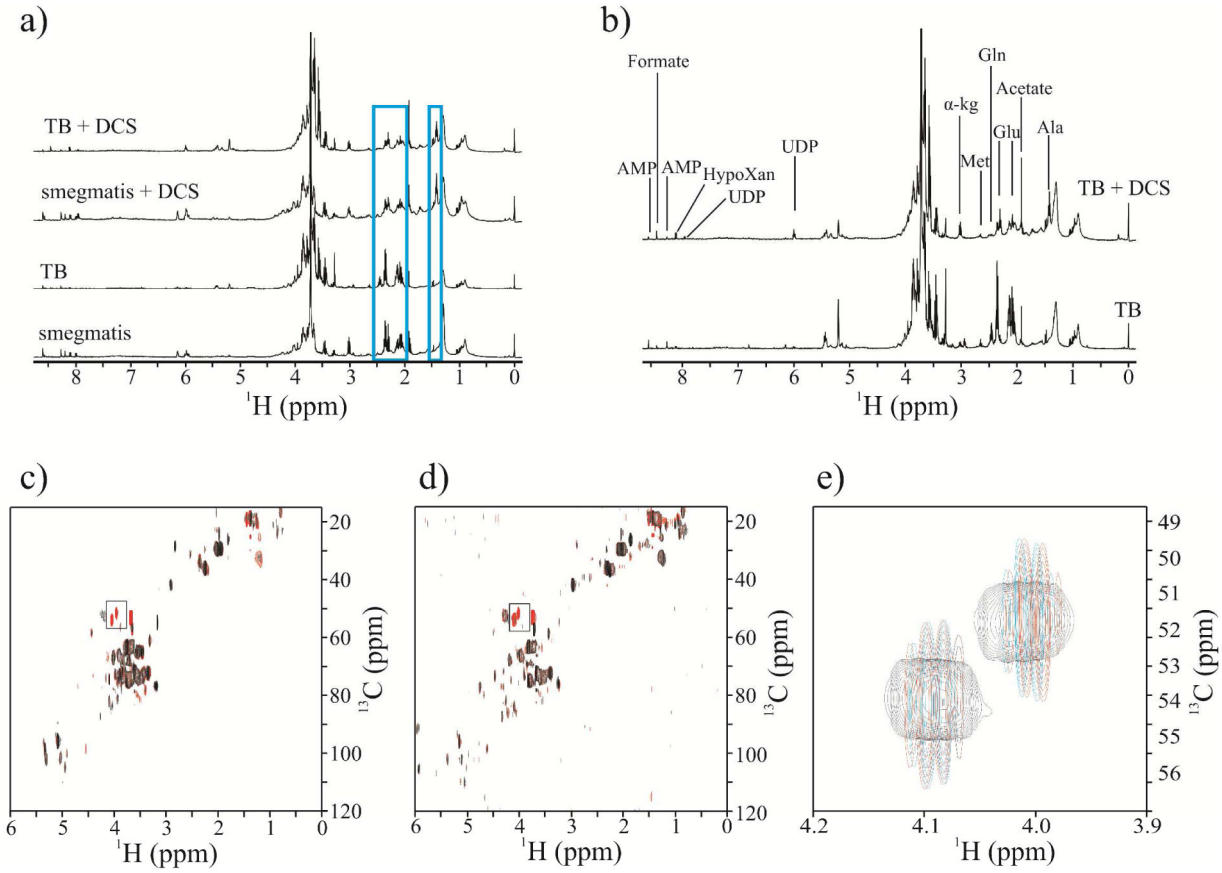

Figure 1.

a) 1D ^{1}H NMR spectra comparing the metabolome of *M. tuberculosis* and *M. smegmatis* with (*top*) and without (*bottom*) treatment with DCS. The highlighted regions show the major differences between the extracted metabolomes when treated with DCS. **b)** The 1D ^{1}H NMR spectra of *M. tuberculosis* with (*top*) and without (*bottom*) treatment with DCS. Key metabolite changes are labeled. Overlay of 2D ^{1}H-^{13}C HSQC spectra comparing metabolite extracts from **c)** *M. tuberculosis* (black) and *M. tuberculosis* treated with 50 μg/mL DCS (red), **d)** *M. smegmatis* (black) and *M. smegmatis* treated with 75 μg/mL DCS (red). The circled region highlights the major differences between the untreated and treated cultures. **e)** Highlighted region of the 2D ^{1}H-^{13}C HSQC spectra comparing *M. tuberculosis* (red) and *M. smegmatis* (blue) treated with DCS, with a reference spectrum of D-alanyl-D-alanine (black).

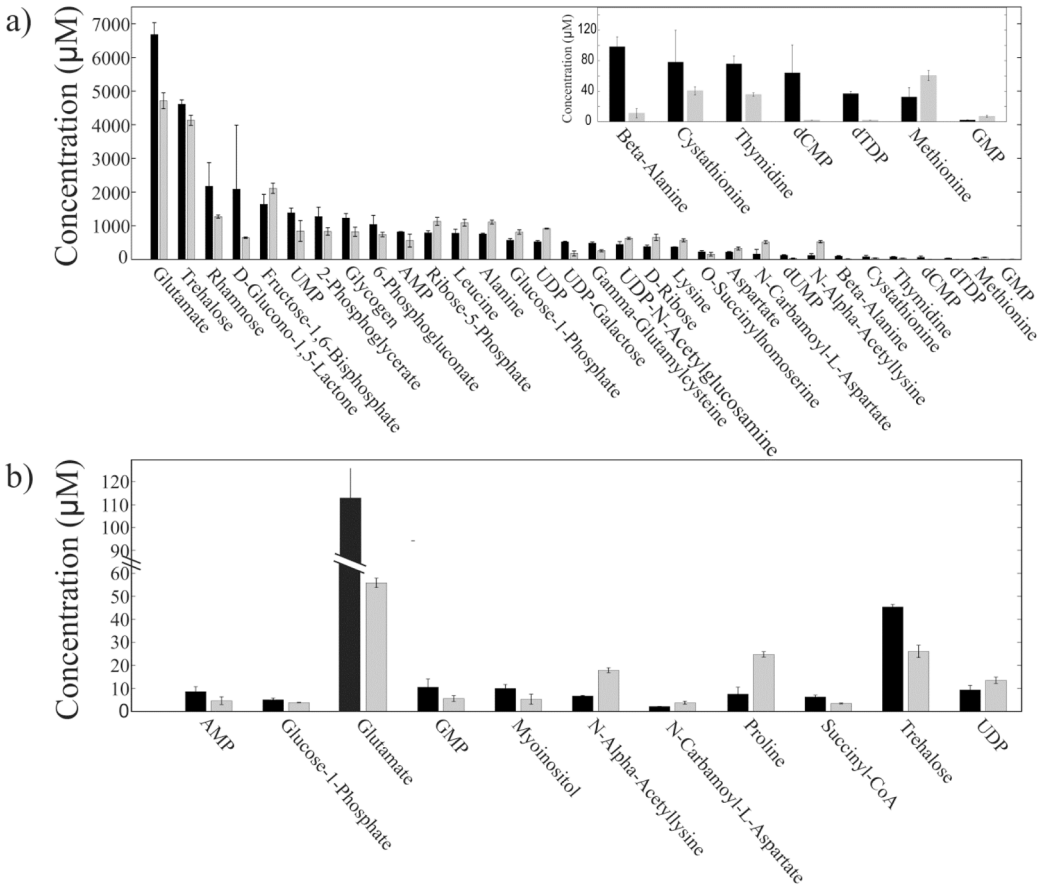

Figure 2.

Bar graphs generated from the average of triplicate 2D ^{1}H-^{13}C HSQC spectra comparing the differences between untreated (black) and DCS treated (white) *M. smegmatis* cultures using **a)** 22 mM ^{13}C-glucose or **b)** 100 μM ^{13}C-pyruvate as the sole carbon-13 source. Metabolites having statistically significant perturbations ($p < 0.05$) upon treatment with DCS are displayed in the bar graph.

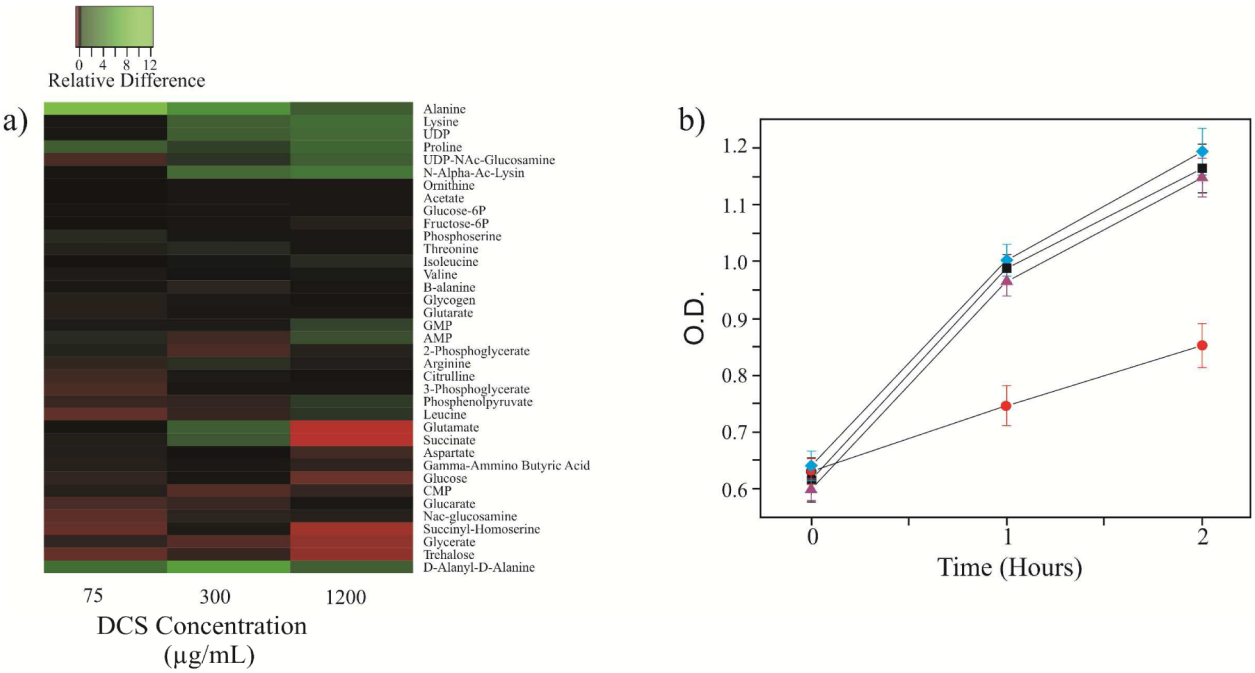

Figure 3.

a) Heat map generated from the average of triplicate $HSQC_0$ spectra comparing the relative difference in metabolite concentrations between *M. smegmatis* and *M. smegmatis* treated with 75, 300, or 1200 μg/mL DCS using 100 μM ^{13}C-D-alanine as the carbon-13 source. The relative differences between the untreated and treated cultures are plotted on a color scale from −100% to −25% (red), −25% to 25% (black), and 25% to 1,200% (green). **b)** *M. smegmatis* growth curve comparing untreated (black) cultures to cultures treated with 75 (magenta), 300 (blue), 1200 μg/mL (red) DCS. O.D values were determined after the treatment of DCS with an initial $O.D._{600}$ of ~0.6.

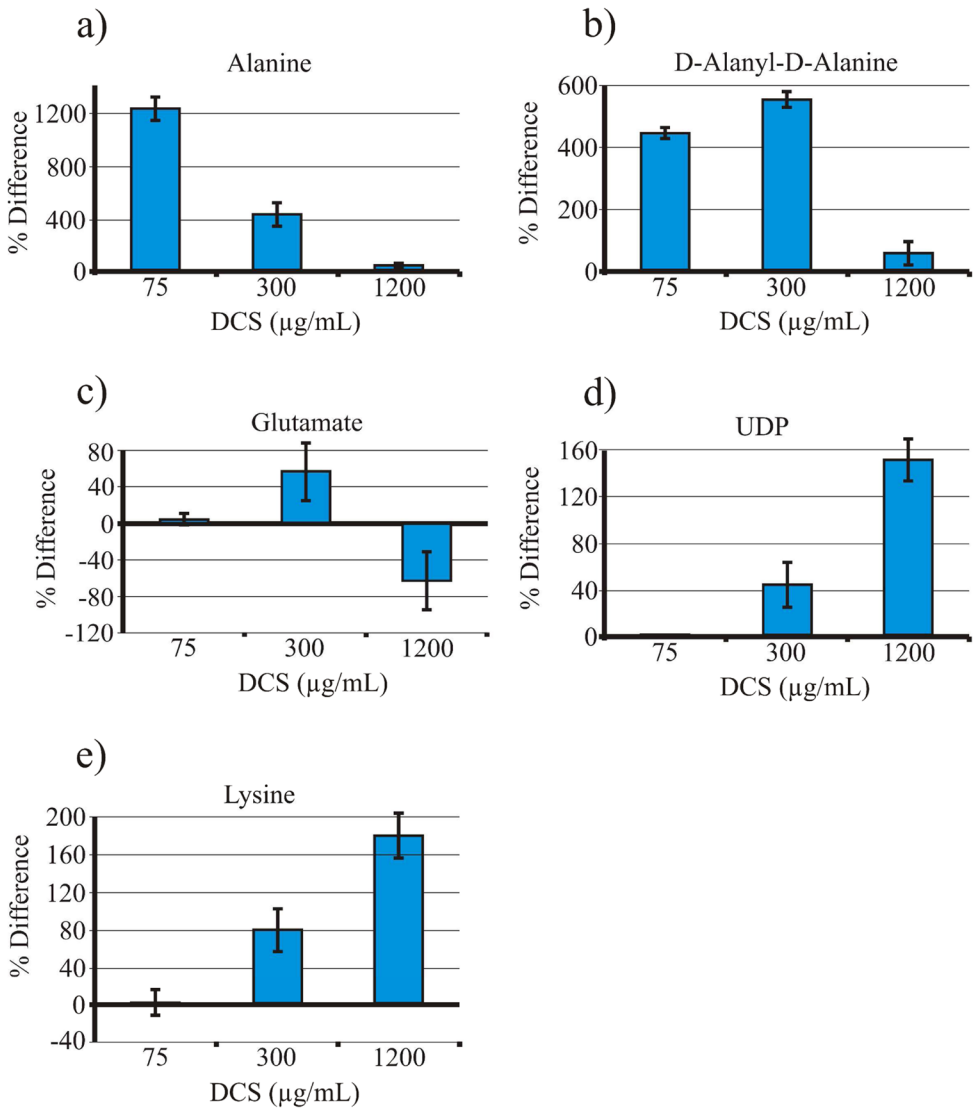

Figure 4.

Bar graphs depicting relative concentration differences in metabolite precursors **a)** alanine, **b)** D-alanyl-D-alanine, **c)** glutamate, **d)** UDP, and **e)** lysine that are involved in the biosynthesis of peptidoglycan. Error bars correspond to standard deviations in the relative concentration differences. The observed metabolite concentration changes result from treating *M. smegmatis* and *M. smegmatis* with DCS. A positive value indicates an increase in the concentration of the metabolites when the cultures are treated with DCS, and a negative value indicates a decrease in the concentration of the metabolites when the cultures are treated with DCS.

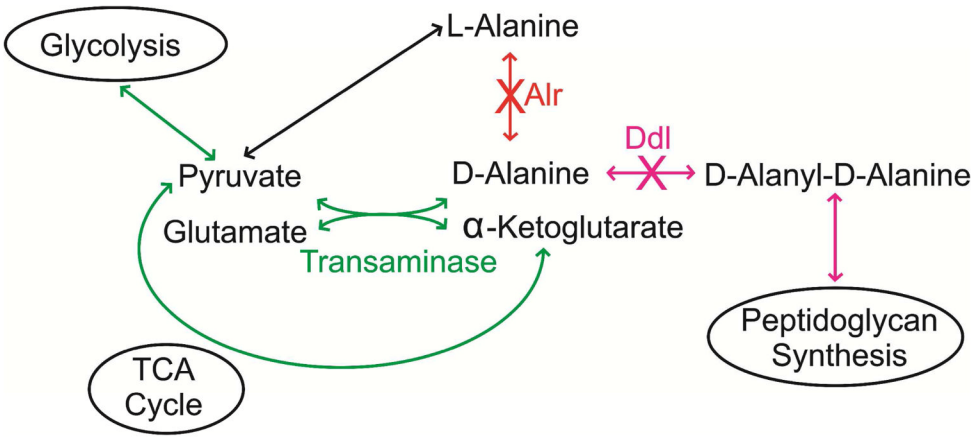

Figure 5.

Schematic representation of pathways that may synthesize D-alanine. Alr (red path) is inhibited at a dose of 75 μg/mL of DCS, which inhibits the primary pathway of D-alanine production. However, inhibiting Alr is non-lethal as a transaminase pathway (green path) is hypothesized to remain unaffected upon DCS treatment. This reaction may lead to an alternative mechanism of D-alanine biosynthesis that antagonizes DCS activity through a competition for Ddl. Ddl (pink path) is inhibited at a dose of 1200 μg/mL of DCS, inhibition of peptidoglycan biosynthesis initiates a cascade of events leading to cell death.[52] TCA, tricarboxylic acid.

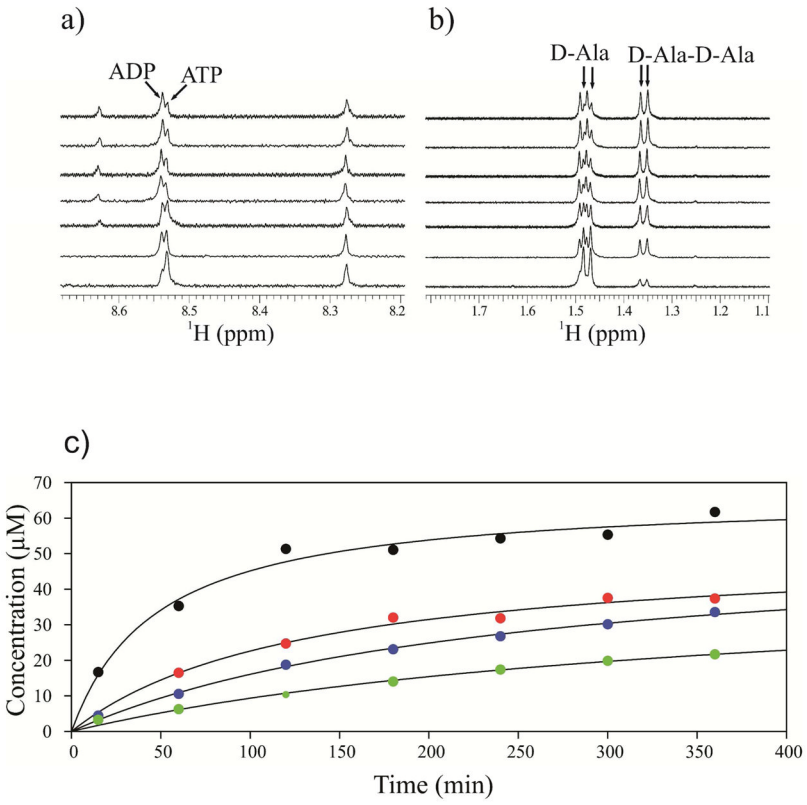

Figure 6.

NMR kinetic analysis of **a)** ADP and **b)** D-alanyl-D-alanine formation by Ddl. The 1D ^{1}H spectrum were collected at one hour intervals after the addition of 25 μM of Ddl into a mixture containing 100 μM D-alanine and 100 μM ATP. **c)** Plot of D-alanyl-D-alanine formation as monitored by 1D ^{1}H NMR that demonstrates a decrease in Ddl activity as a function of increasing DCS concentration: 0 (black), 250 (red), 500 (blue), 1000 (green) μM of DCS.

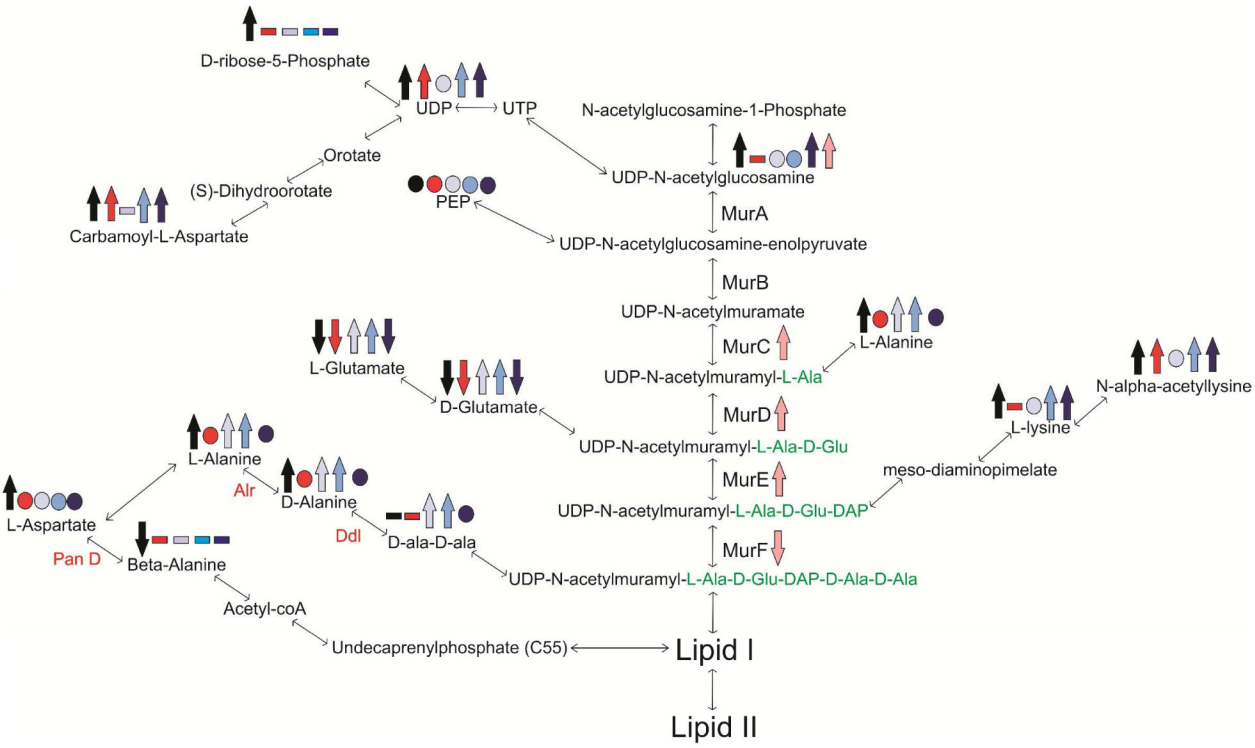

Figure 7.

Peptidoglycan biosynthesis pathway depicting the metabolites that were identified by 2D ^{1}H-^{13}C HSQC analysis or from literature results.[53, 54] The arrows correspond to metabolites with statistically significant ($p < 0.05$) concentration increases (up) or decreases (down) when comparing DCS treated cells to untreated cells. Circles indicate the metabolite concentration is similar ($p > 0.05$). The p values were calculated using the Student's t-test. Hyphens indicate the metabolites were not identified for the specific carbon-13 source. Cells were incubated with ^{13}C-glucose and treated with 75 μg/mL of DCS (black arrow), ^{13}C-pyruvate and treated with 75 μg/mL of DCS (red arrow), ^{13}C-alanine and treated with 75 μg/mL of DCS (grey arrow), ^{13}C-alanine and treated with 300 μg/mL of DCS (blue arrow), ^{13}C-alanine and treated with 1200 μg/mL of DCS (dark blue arrow), and literature data (pink arrows)

Table 1

Transaminase Activities Identified in *M. smegmatis* and *M. tuberculosis*[1]

Enzyme Name	EC Number	*M. smegmatis* ORF	*M. tuberculosis* ORF	Catalyzed Reaction
Probable Aspartate transaminase (AspB)	2.6.1.1	MSMEG_6017	Rv3565	L-aspartate + α-ketoglutarate --- oxaloacetate + L-glutamate
Probable Aspartate or Alanine transaminase (AspC)	2.6.1.1 or 2.6.1.2	MSMEG_0688	Rv0337c	L-aspartate + α-ketoglutarate --- oxaloacetate + L-glutamate ***or*** L-alanine + α-ketoglutarate --- pyruvate + L-glutamate
4-Aminobutyrate-2-oxoglutarate transaminase (GabT)	2.6.1.19	MSMEG_2959	Rv2589	γ-aminobutyrate + α-ketoglutarate --- succinate semialdehyde + L-glutamate
D-amino acid transaminase (D-Alanine transaminase)	2.6.1.21	None identified	None identified	D-alanine + α-ketoglutarate --- pyruvate + D-glutamate
Branched-chain amino acid transaminase (IlvE)	2.6.1.42	MSMEG_4276	Rv2210c	L-leucine + α-ketoglutarate ---- α-ketoisocaproate + L-glutamate

[1]Output based on Tuberculist database (http://tuberculist.epfl.ch/)[51]